

# Alkoxide Route to Mixed Oxides of Rhenium, Niobium, and Tantalum. Preparation and X-ray Single-Crystal Study of a Novel Rhenium–Niobium Methoxo Complex, $\text{Nb}_2(\text{OMe})_8(\text{ReO}_4)_2$

Pavel A. Shcheglov and Dmitry V. Drobot

*Moscow State Academy of Fine Chemical Technology. Pr. Vernadskogo 86, 117571 Moscow, Russia*

Gulaim A. Seisenbaeva, Suresh Gohil, and Vadim G. Kessler\*

*Department of Chemistry, Swedish University of Agricultural Sciences (SLU), Box 7015, 75007 Uppsala, Sweden*

Received December 20, 2001. Revised Manuscript Received March 13, 2002

Thermal decomposition of complex oxomethoxo compounds  $\text{Nb}_4\text{O}_2(\text{OMe})_{14}(\text{ReO}_4)_2$  (**I**) and  $\text{Ta}_4\text{O}_2(\text{OMe})_{14}(\text{ReO}_4)_2$  (**II**) has been investigated. The decomposition of (**II**) at temperatures exceeding 100 °C results in the formation of  $\text{MeOMe}$ ,  $\text{MeOCH}_2\text{OMe}$ ,  $\text{MeOH}$ , and  $\text{H}_2\text{O}$  vapor and is accompanied by sublimation at temperatures over 135 °C. Plausible mechanisms of the processes studied are discussed. A new bimetallic methoxo compound,  $\text{Nb}_2(\text{OMe})_8(\text{ReO}_4)_2$  (**III**), was synthesized by interaction between  $\text{Re}_2\text{O}_7$  and  $\text{Nb}_2(\text{OMe})_{10}$  in toluene solution and its structure was determined by means of an X-ray single-crystal study. The structure can be considered as a product of substitution for terminal methoxo groups with two perrhenate groups in dimeric  $\text{Nb}_2(\text{OMe})_{10}$  molecules. Decomposition of **II** in an inert atmosphere at 900 °C gave a Re–Ta mixed oxide phase, supposedly based on the  $\text{L-Ta}_2\text{O}_5$  structure. Decomposition of **I** and **III** under similar conditions leads to the formation of rhenium–niobium oxide phases. The results obtained provide a basis for the alkoxide approach to the synthesis of oxide and metallic rhenium-based materials.

## Introduction

Rhenium-based oxide materials are of substantial interest both as components of catalysts and as intermediate products in the preparation of fine rhenium metal and alloy powders.<sup>1</sup>

The application of individual and bimetallic alkoxy derivatives as precursors proved to be promising in the preparation of rhenium-based oxide materials. This approach permits one to obtain materials possessing the required microstructure, chemical composition, and degree of chemical and phase homogeneity at relatively low temperatures.<sup>2</sup>

We have recently reported the synthesis and characterization of  $\text{Nb}_4\text{O}_2(\text{OMe})_{14}(\text{ReO}_4)_2$  (**I**) and  $\text{Ta}_4\text{O}_2(\text{OMe})_{14}(\text{ReO}_4)_2$  (**II**)—prospective molecular precursors of Re-based materials. The determination of their structures by an X-ray single-crystal study showed these complexes to be built up of the planar tetrานuclear  $\text{M}_4(\mu\text{-O})_2(\mu\text{-OMe})_4$  core ( $\text{M} = \text{Nb}$  or  $\text{Ta}$ ).<sup>3,4</sup> To complete the octahe-

dral coordination of the metal atoms, there are 10 terminal methoxo groups and two perrhenate groups bonded to the metal atoms.

The decomposition behavior of  $\text{Nb}_4\text{O}_2(\text{OMe})_{14}(\text{ReO}_4)_2$  (**I**) and  $\text{Ta}_4\text{O}_2(\text{OMe})_{14}(\text{ReO}_4)_2$  (**II**) has not been investigated so far. We were interested in investigating the nature of the processes taking place on thermal treatment of these compounds and also look for the possibility of obtaining heterometallic precursors with chemical compositions different from those studied so far.

## Experimental Section

All of the preparative procedures were carried out in a dry nitrogen atmosphere using a drybox. Methanol was purified and dehydrated by refluxing over magnesium methoxide with subsequent distillation. Toluene was distilled after refluxing with metallic sodium.

IR spectra of Nujol mulls were obtained with a Perkin-Elmer FT-IR 1720 X spectrometer. The  $^1\text{H}$  NMR spectrum solution was obtained with a Varian 400-MHz spectrometer (undehydrated toluene was used as the solvent). Thermogravimetric analysis (TGA) in a nitrogen atmosphere (heating rate, 10 °C/min) was performed with a Perkin-Elmer TGA-7 analyzer. The metal ratio in the samples was determined by means of a JEOL JSM-820 scanning microscope (SEM), supplied with a Link AN-10000 energy-dispersive spectrometer (EDS). TGA

(1) Forde, P. T. *Rhenium and Rhenium Alloys. Proceedings of the International Symposium*, Feb 10–13, 1997; Bryskin, B. D., Ed.; Minerals, Metals, Material Society (TMS), 1977, p 755.

(2) Seisenbaeva, G. A.; Kessler, V. G.; Sundberg, M.; Nygren, M.; Drobot, D. V. *Rhenium and Rhenium Alloys. Proceedings of the International Symposium*, Feb 10–13, 1997; Bryskin, B. D., Ed.; Publ. TMS, p 159.

(3) Seisenbaeva, G. A.; Shevelkov, A. V.; Tegenfeldt, J.; Klo, L.; Drobot, D. V.; Kessler, V. G. *Dalton Trans.* **2001**, 2762.

(4) Seisenbaeva, G. A.; Kessler, V. G.; Shevelkov, A. V. *J. Sol–Gel Sci. Technol.* **2000**, 19, 285.

and SEM-EDS experiments were carried out at Arrhenius Laboratory, Stockholm University.

The decomposition and sublimation processes in a vacuum were studied using a Schlenk line evacuated by a rotatory oil pump ( $p = 10^{-2}$  mmHg). The substance under study was heat-treated in a glass vessel (20–200 °C, 20 °C/min), and during the course of decomposition, the gaseous products were collected in a trap cooled with liquid nitrogen. After the decomposition process was completed, the system was filled with dry nitrogen and, after warming to room temperature, a sample of gas phase from the trap was investigated by GC-MS using a Hewlett-Packard 5890 Series II gas chromatograph supplied with a capillary separative column with DB-Wax film phase (manufactured by J&W Scientific, CA) and coupled with a JEOL JMS-SX/SX102A Tandem mass spectrometer (electron beam ionization, direct probe introduction).

X-ray powder diffraction patterns were obtained by Mr. Lars Göthe at Stockholm University using the Guinier–Hägg technique.

The determination of carbon and hydrogen contents was carried out by Mikrokemi AB, Uppsala, Sweden, using conventional organic microanalysis technique.

The alkoxides,  $\text{Nb}_2(\text{OMe})_{10}$  and  $\text{Ta}_2(\text{OMe})_{10}$ , used in this work as starting materials for the synthesis of bimetallic complexes, were prepared by anodic oxidation of the corresponding metals in methanol and purified according to conventional techniques.<sup>3–5</sup> Rhenium(VII) oxide (99.9+%) was purchased from Aldrich. The identity of synthesized samples of **I**, **II**, and **III** with investigated single crystals was established via a comparison of experimental XRD powder patterns with the theoretical ones calculated using single-crystal data (the latter are available as Supporting Information).

**Synthesis.**  $\text{Nb}_4\text{O}_2(\text{OMe})_{14}(\text{ReO}_4)_2$  (**I**) and  $\text{Ta}_4\text{O}_2(\text{OMe})_{14}(\text{ReO}_4)_2$  (**II**). **I** and **II** were synthesized according to recently developed techniques<sup>3</sup> via interaction of  $\text{Nb}_2(\text{OMe})_{10}$  or  $\text{Ta}_2(\text{OMe})_{10}$  with  $\text{Re}_2\text{O}_7$  in toluene.

$\text{Nb}_2(\text{OMe})_8(\text{ReO}_4)_2$  (**III**). The compound **I** is poorly soluble in toluene and contains tetrameric structure units possessing relatively high stability,<sup>3</sup> so it seemed to be unexpedient to use the reaction of **I** with further amounts of solid  $\text{Re}_2\text{O}_7$  to obtain possible products with increased Re/Nb ratio. We chose instead to introduce an increased amount of  $\text{Re}_2\text{O}_7$  at the initial step of the synthesis.  $\text{Re}_2\text{O}_7$  (1.151 g, 2.38 mmol) was added to the solution of  $\text{Nb}_2(\text{OMe})_{10}$  (0.590 g, 1.19 mmol) in 7 mL of toluene upon stirring. No color changes were observed after the addition of the first portions of  $\text{Re}_2\text{O}_7$ . In the course of further addition of  $\text{Re}_2\text{O}_7$ , the solution became brownish pink. This color change was accompanied by the formation of light pink crystals and deposition of a black dense product on the bottom of the flask. The mixture obtained was heated slightly to  $\approx 50$  °C. The black dense precipitate at the bottom of the flask was isolated by decantation. The warm mother liquor was cooled to room temperature and then to  $-30$  °C in a freezer. After 3 days the solution was decanted and the remaining crystalline product was dried in a vacuum. Yield ca. 30% with respect to  $\text{Re}_2\text{O}_7$ . Found, %: C, 9.80; H, 2.30. Nb:Re = 1:1. Calculated for  $\text{Nb}_2(\text{OMe})_8(\text{ReO}_4)_2$ , %: C, 10.28; H, 2.59. IR,  $\text{cm}^{-1}$ : 1123 s, 1073 s, 1002 m, 970 w, 943 s, 935 s, 856 m, 780 w sh, 739 w, 666 w, 574 s, 524 s. NMR  $^1\text{H}$  ( $\text{CDCl}_3$ ), ppm: 4.25 (2H,  $\text{CH}_3$ ), 4.20 (4H,  $\text{CH}_3$ ), 3.97 (2H,  $\text{CH}_3$ ). Mass spectrum (for rhenium-containing species,  $m/z$  values are reported in relation to the  $^{187}\text{Re}$  isotope),  $m/z$  (I, %): 465 (1.3)  $\text{Nb}_2(\text{OMe})_9^+$ ; 434 (0.6)  $\text{Nb}_2(\text{OMe})_8^+$ ; 419 (0.3)  $\text{Nb}_2(\text{OMe})_7^+$ ; 403 (1.0)  $\text{Nb}_2(\text{OMe})_6^+$ ; 388 (0.5)  $\text{Nb}_2\text{O}(\text{OMe})_6^+$ ; 373 (0.5)  $\text{Nb}_2\text{O}_2(\text{OMe})_5^+$ ; 372 (0.3)  $\text{Nb}_2(\text{OMe})_6^+$ ; 266 (62)  $\text{ReO}_3(\text{OMe})^+$ ; 236 (100)  $\text{ReO}_2(\text{OH})^+$ ; 219 (61)  $\text{ReO}_2^+$ ; 217 (50)  $\text{Nb}(\text{OMe})_4^+$ ; 203 (22)  $\text{ReO}^+$ ; 187 (11)  $\text{NbO}_2(\text{OR})_2^+$ ,  $\text{Re}^+$ ; 186 (2.0)  $\text{Nb}(\text{OMe})_3^+$ ; 185 (12)  $\text{Nb}(\text{OMe})_2\text{OCH}_2^+$ ; 155 (2.5)  $\text{Nb}(\text{OMe})_2^+$ ; 124 (2.0)  $\text{Nb}(\text{OMe})^+$ .

**Crystallography.**  $\text{C}_8\text{H}_{24}\text{Nb}_2\text{O}_{16}\text{Re}_2$ ,  $M = 934.49$ . Monoclinic, space group  $P2(1)/c$ ,  $a = 8.5609(16)$  Å,  $b = 12.890(3)$  Å,

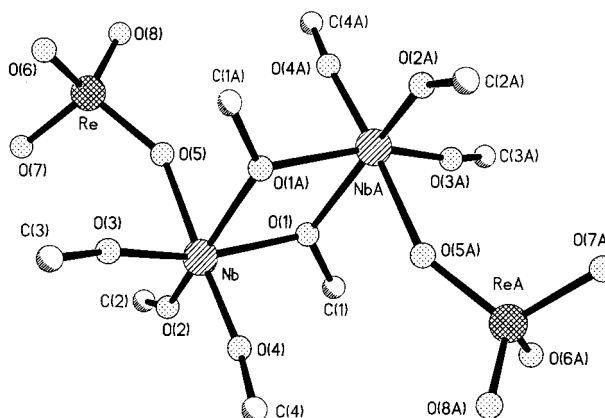


**Figure 1.** Molecular structure of  $\text{Nb}_2(\text{OMe})_8(\text{ReO}_4)_2$  (**III**).

$c = 10.652(3)$  Å,  $\beta = 97.31(3)$  °,  $V = 1165.9(5)$  Å<sup>3</sup>,  $D_{\text{calc}} = 2.662$  g/cm<sup>3</sup> for  $Z = 2$ ,  $\lambda(\text{Mo K}\alpha) = 0.71073$  Å. A total of 1079 [R(int) = 0.11144] independent reflections with  $I > 2\sigma(I)$  were collected at 20 °C up to  $2\theta_{\text{max}} = 40.00$  ° (the completeness 98.9%). Data collection was performed using a Bruker SMART CCD 1K diffractometer. SAINT PLUS and SHELXTL-NT program packages were used for data reduction and computations. Empirical absorption correction was applied ( $\mu = 11.371$  mm<sup>-1</sup>) using the Bruker SADABS program package. The structure was solved by direct methods. The coordinates of heavy atoms were taken from the initial solution. The other non-hydrogen atoms were located in subsequent Fourier syntheses. The structure was refined by full-matrix least-squares on  $F^2$  in an isotropic and then in an anisotropic approximation. The positions of terminal oxygen atoms of perrhenate groups subjected to some degree of rotational disorder were refined using geometrical restraints to support idealized tetrahedral geometry. The positions of the hydrogen atoms were calculated geometrically and included in the final cycles of refinement in an isotropic approximation. The final discrepancy factors are  $R_1 = 0.0585$  and  $wR_2 = 0.1200$ . The highest difference peak (1.651 e·Å<sup>-3</sup>) is located near the rhenium atom (at 1.08 Å) and the deepest hole (−0.980 e·Å<sup>-3</sup>) is located at 0.86 Å from one of the terminal oxygen atoms of the  $\text{ReO}_4$  group.

## Results and Discussion

The centrosymmetric molecule of  $\text{Nb}_2(\text{OMe})_8(\text{ReO}_4)_2$  (**III**) contains a pair of niobium atoms connected via two bridging methoxide groups (Figure 1). The octahedral coordination of each niobium atom is completed by three terminal methoxide groups (two in the equatorial position and one in the axial position) and one perrhenate group, bonded through a bridging oxygen atom. In terms of the coordination polyhedra, this molecule comprises two edge-sharing  $\text{NbO}_6$  octahedra and two  $\text{ReO}_4$  tetrahedra, sharing corners with each  $\text{NbO}_6$  octahedron. The  $\text{NbO}_6$  octahedra are significantly distorted with O–Nb–O angles between vicinal oxygen atoms lying within the range of 70.6(6)–104.6(7)°.

The structure of **III** can be derived from that of **I** (Figure 2) by cleavage of the two Nb–(μ-O) bonds in the tetrameric  $\text{Nb}_4(\mu\text{-O})_2(\mu\text{-OMe})_4$  fragment to form the dimeric  $\text{Nb}(\mu\text{-OMe})_2\text{Nb}$  fragments and by further replacement of the bridging oxo ligand with the  $\text{ReO}_4$  group at the niobium atom that did not bear it before and with a methoxide group at the other niobium atom. The structure of **III** can also be treated as derived from the dimeric structure of  $\text{Nb}_2(\text{OMe})_{10}$  by simple substitution for the terminal methoxo ligands with two perrhenate groups at each niobium atom in the axial positions.

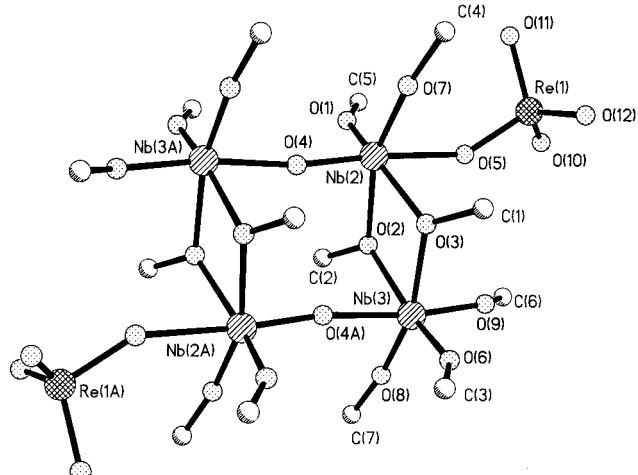


**Figure 2.** Molecular structure of  $\text{Nb}_4\text{O}_2(\text{OMe})_{14}(\text{ReO}_4)_2$  (**I**).<sup>3</sup>

The geometrical features of **III** are rather close to that of  $\text{Nb}_2(\text{OMe})_{10}$ .<sup>6</sup>

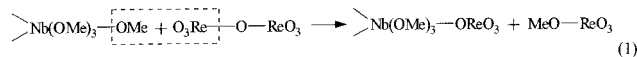
The distances between the niobium and the oxygen atoms of the terminal methoxy groups (1.811(14)–1.819(17) Å) are nearly the same as those in the structure of **I** (1.804(7)–1.852(8) Å) and are slightly shorter compared to those of  $\text{Nb}_2(\text{OMe})_{10}$  (1.875(5)–1.912(8) Å). Taking into consideration the estimated standard deviations of bond lengths, the latter difference can be considered as significant and this allows us to suggest that the decrease in the Nb–O bond lengths for the terminal methoxy groups indicates the increased degree of the Nb–O  $\pi$ -bonding. In the structure of  $\text{Nb}_2(\text{OMe})_{10}$  the 16 electrons of the 4 oxygen atoms of the terminal OMe groups are potentially available for the  $d_{\pi} \leftarrow p_{\pi}$  interaction with the three empty  $t_{2g}$  orbitals of each Nb atom.<sup>6</sup> The substitution for one terminal methoxy group bonded to the Nb atom with one perrhenate group should lead to the increase in  $\pi$ -bonding contribution for each oxygen atom belonging to the remaining terminal OMe groups because the oxygen atom of the perrhenate group is unable to contribute to the Nb–O  $\pi$ -bonding, as evidenced by the rather long corresponding bond distance (2.162(15) Å).

The distances between the niobium atoms and the oxygen atoms belonging to the bridging methoxy groups are within the ordinary limits: 2.060(13) and 2.127(14) Å compared to 2.084(6)–2.097(6) Å for **II** and 2.114(7)–2.149(6) Å for  $\text{Nb}_2(\text{OMe})_{10}$ .

The IR spectrum for **III** is consistent with the molecular structure described above. The vibrations in the region of 943–945  $\text{cm}^{-1}$  could be assigned to the  $\nu(\text{Re}=\text{O})$  in the  $\text{ReO}_4$  tetrahedra; the band at 1073  $\text{cm}^{-1}$  corresponds to the  $\nu(\text{C}-\text{O})$ , while the bands at 574 and 524  $\text{cm}^{-1}$  may be assigned to the  $\nu(\text{Nb}-\text{OMe})$  vibrations for the terminal and the bridging methoxy groups, respectively. The  $^1\text{H}$  NMR spectrum of **III** indicates that the molecular structure observed in the solid state is preserved in solution as the intensity ratio 2:4:2 corresponds to the functions of the methoxide groups (2 bridging, 4 terminal equatorial, and 2 terminal axial) in the molecular structure revealed by the X-ray single-crystal study.

(6) Pinkerton, A. A.; Schwarzenbach, D.; Hubert-Pfalzgraf, L. G.; Riess, J. G. *Inorg. Chem.* **1976**, *15* (5), 1196.

Taking into consideration the structural features of the initial compounds,  $\text{Nb}_2(\text{OMe})_{10}$  and  $\text{Re}_2\text{O}_7$ , the formation of **III** with the structure described above is quite reasonable. The rhenium(VII) oxide does not possess the molecular type of structure, but strong distortion of the coordination polyhedra brings about the formation of relatively short and long ( $>2$  Å) Re–O bonds. Because of these long Re–O bonds, the  $\text{ReO}_3$ –O– $\text{ReO}_3$  molecular species are easily generated upon reactions with solid  $\text{Re}_2\text{O}_7$ .<sup>7</sup>  $\text{Re}_2\text{O}_7$  can react with the compounds containing methoxide groups. The  $\text{Nb}(\mu\text{-OMe})_2\text{Nb}$  fragments, typical for the  $\text{Nb}_2(\text{OMe})_{10}$  structure, remain unchanged (eq 1).



The rhenium(VII) monomethoxide, formed supposedly as the major byproduct in this reaction, is unstable under normal conditions because of the oxidizing properties of Re(VII) centers in relation to the bonded methoxy group and decomposes forming black solid products.<sup>8</sup> Thus, the observed deposition of the black product during the synthesis of **III**, together with the observed yields of <50% with respect to  $\text{Re}_2\text{O}_7$ , support the proposed mechanism.

The mechanism of formation of the complexes **I** and **II** is evidently more complicated. The reduced  $\text{Re}_2\text{O}_7$  amount introduced into reaction probably causes the formation of  $(\text{MeO})_4\text{M}(\mu\text{-OMe})_2\text{M}(\text{OMe})_3-\text{ReO}_3$  molecular species with the Re:M = 1:2, M = Nb or Ta, which undergo further dimerization with formation of the oxo bridges. The formation of the two different structures upon introduction of different amounts of  $\text{Re}_2\text{O}_7$  is thus in accordance with the supposed mechanism. Generally, the process mechanisms are rather intricate for the reactions of the alkoxide complexes, but the formation of a definite crystalline product is usually favored by its high relative thermodynamical stability and low solubility under the conditions applied.

The investigation of the thermal properties of **II** in a vacuum showed the deposition of two different products on the cool parts of the glass vessel at the initial stage (135 °C) of the sublimation process, namely, the white film of the less volatile product and the reddish purple one of the more volatile product. The latter became dark upon further heating and resembled the sublimation product of  $\text{Re}_4\text{O}_6(\text{OMe})_{12}$ .<sup>3,4,9</sup> The formation of two different sublimation products should have occurred through the separation of rhenium- and tantalum-containing volatile methoxide species upon the decomposition of the complex compound **II**. Upon further heating of the solid residue, the formation of a liquid phase was observed at 145 °C and its “boiling” started at 150 °C. The liquid phase was then converted into a black solid residue at 165 °C. The solid residue was found amorphous according to the X-ray diffraction study.

The occurrence of the competition between the sublimation and the decomposition observed here appears

(7) Krebs, B.; Muller, A.; Beyer, H. H. *Inorg. Chem.* **1969**, *8*, 436.

(8) Edwards, P. G.; Wilkinson, G. *J. Chem. Soc., Dalton Trans.* **1984**, 2695.

(9) Seisenbaeva, G. A.; Sundberg, M.; Nygren, M.; Dubrovinsky, L.; Kessler, V. G., to be published.

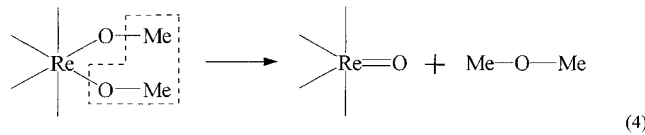
similar to the behavior of the individual rhenium oxomethoxide  $\text{Re}_4\text{O}_6(\text{OMe})_{12}$ . (In the latter case the thermal decomposition at temperatures exceeding 100 °C is accompanied by sublimation over 140 °C.<sup>4</sup>) The analogy in the sublimation behavior of these compounds concerns also the absence of the structural units, found for the solid state, in the gas phase. For  $\text{Re}_4\text{O}_6(\text{OMe})_{12}$  we suggested the splitting of the tetrameric molecules into  $\text{Re}_2\text{O}_3(\text{OMe})_6$  dimers that upon further decomposition were converted into the monomeric species in the vapor phase (eqs 2 and 3).



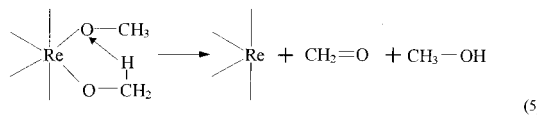
Dissociation into the homometallic fragments occurs also for the molecules of **III** as evidenced by its mass spectrum, which contains no fragmentation series for the bimetallic species.

According to the GC-MS study (Figure 3), the gaseous products formed in the course of heating are dimethyl ether, dimethylacetal, methanol, and water. As the synthesis of **II** was performed in toluene, this compound was also detected due to occlusion and the absorption of toluene by the crystals of **II**. It can be noted that as in the case of the homometallic rhenium oxomethoxide,  $\text{Re}_4\text{O}_6(\text{OMe})_{12}$ , the formation of the same products is observed in comparable quantities.<sup>4</sup>

The presence of the dimethyl ether indicates that the ether elimination mechanism contributes to the decomposition process. This mechanism is known to occur in the case of molybdenum and tungsten alkoxy derivatives<sup>10</sup> and can be schematically presented as eq 4.



We can consider the presence of methanol as an indication of the  $\beta$ -H elimination mechanism, which was previously observed for the rhenium(V) oxo-alkoxide complexes.<sup>11</sup> Another product of this process must be the formaldehyde according to the scheme in eq 5.



The absence of this compound among the decomposition products together with the presence of a considerable amount of its dimethylacetal permit us to suppose that the formaldehyde should undergo the transformation into the acetal. It was in fact found earlier that the molybdenum alkoxides induce such rapid conversion of carbonyl compounds into acetals.<sup>12</sup> This can explain also the absence of the formic acid or its ester (in the case of  $\text{Re}_4\text{O}_6(\text{OMe})_{12}$  methyl formate is found only in minor

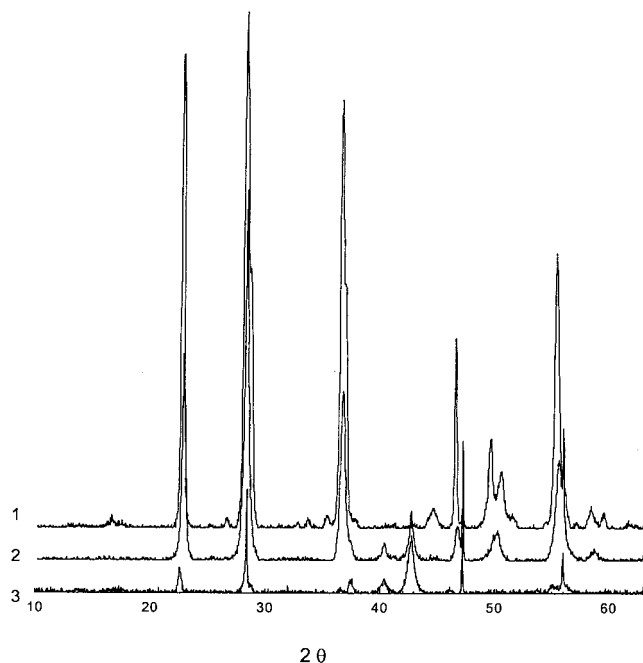


**Figure 3.** X-ray powder patterns of the decomposition products of **I**(1), **II**(2), and **III**(3) in a nitrogen atmosphere at 900 °C.

quantities, several times the detectability limit), which could be expected as the products of the transformation of the formaldehyde via Tishchenko reaction among the decomposition products, as the rapid conversion of the formaldehyde into the acetal prevents such transformation.

In the earlier studies of the thermal behavior of the molybdenum and tungsten alkoxides,  $\text{M}_2(\text{OR})_6$  and  $\text{M}_2(\text{CH}_2\text{Ph})_2(\text{OR})_4$ ,  $\text{R} = \text{Pr}^i, \text{Bu}^t$ , the presence of acetals was not detected in contrast to our studies, and the main products were found to be the corresponding hydrocarbons, alcohols, and acetone.<sup>13</sup> The authors suggested the mechanism including the formation of the carbenium ion (6) as the initial stage of the decomposition.



This reaction can be considered as the main common feature with the mechanism suggested in this work (4), as the initial stage of the ether elimination process includes also the formation of a carbocation. Further transformation pathways are quite different, apparently, because of the essential difference in the nature of the alkoxo ligands in question, which leads to the significant difference in the gaseous products formed.

Thus, the decomposition experiments reveal an analogy in the mechanisms of the decomposition of the bimetallic tantalum–rhenium compound **II** and the homometallic rhenium methoxide,  $\text{Re}_4\text{O}_6(\text{OMe})_{12}$ . The data obtained confirm the main reaction pathways to be the ether elimination reaction found previously for the molybdenum and tungsten alkoxides, in combination with the  $\beta$ -H elimination reaction, observed earlier for the rhenium alkoxide compounds. In addition, we can suppose now that the catalytical action of the alkoxide complexes on the carbonyl compounds results

(10) Turova, N. Ya.; Kessler, V. G.; Kuchekko, S. I. *Polyhedron* **1991**, *10*, 2617.

(11) DuMez, D. D.; Mayer, J. M. *Inorg. Chem.* **1995**, *34*, 6396.

(12) Kessler, V. G.; Nikitin, K. V.; Belokon, A. I. *Polyhedron* **1998**, *17*, 2309.

(13) Baxter, D. V.; Chisholm, M. H.; Distasi, V. F.; Haubrich, S. T. *Chem. Mater.* **1995**, *7*, 84.

**Table 1. Thermal Decomposition Behavior of Obtained Oxomethoxo Compounds**

investigated sample	conditions: temperature and atmosphere	decomposition stages: temperature and mass loss	phase composition of final decomposition product	further details
<b>II</b>	RT → 700 °C, air	Δm = 45%	amorphous phase	light gray in color; Re/(Re + Ta) = 6.2–6.7 at. %
	RT → 900 °C, air	Δm = 48%	monophase rhenium-doped "L-Ta <sub>2</sub> O <sub>5</sub> " (orthorhombic low-temperature phase)	pale yellow in color; Re/(Re + Ta) = 2.3–2.5 at. %
	RT → 900 °C, N <sub>2</sub>	150–317 °C (Δm = 20.7%) 812–870 °C (Δm = 23.6–27.1%)	amorphous after first step crystalline rhenium–tantalum oxide phase after second step	gray in color with metallic luster; Re/(Re + Ta) = 23.7–25.1 at. % after second step
<b>III</b>	RT → 900 °C, N <sub>2</sub>	170–218 °C (Δm = 14.8%) 251–317 °C (Δm = 22.5%) 581–647 °C (Δm = 27.1%) 746– not finished at 900 °C (Δm = 28.5–33.0% at 880 °C)	rhenium–niobium oxide phase	gray in color with metallic luster.
	RT → 900 °C, air		"H-Nb <sub>2</sub> O <sub>5</sub> " with admixtures of low-temperature phases	white in color

in the formation of the acetals, as was found previously for the molybdenum alkoxide compounds.

The investigation of the decomposition process for the compound **II** showed that the heat treatment in air at 700 and 900 °C led to the mass loss values comparable to the calculated ones, assuming the product to be rhenium-free Ta<sub>2</sub>O<sub>5</sub> (47.7%) (Table 1). This implies that the samples have lost almost all rhenium in the form of the highly volatile Re<sub>2</sub>O<sub>7</sub> (a small rhenium amount being still present in the product according to EDS analysis). Taking into consideration the high temperature of the heat treatment and the fact that the homometallic rhenium oxides undergo oxidation in air at temperatures above 400 °C to form the highly volatile Re<sub>2</sub>O<sub>7</sub> (which has as low a boiling point as 360 °C), the presence of rhenium in the form of the homometallic rhenium oxides should be excluded. The X-ray powder diffraction pattern of the product treated at 900 °C corresponds to that of the low-temperature orthorhombic modification of the L-Ta<sub>2</sub>O<sub>5</sub> phase, and the unit cell parameters calculated for the experimental pattern by the least-squares technique are close to the values reported in the reference data.<sup>14</sup>

Heat treatment in an inert atmosphere results in the formation of a complex rhenium–tantalum oxide phase. According to the TGA study, upon decomposition of **II** in an inert atmosphere there are two well-defined mass loss steps. The first one is evidently associated with the decomposition process itself. The mass loss after the first step is close to the calculated value, assuming the product of the decomposition to be Re<sub>2</sub>Ta<sub>4</sub>O<sub>16</sub> (20.0%). X-ray powder analysis showed the product after the first stage of decomposition and after its subsequent heating to 750 °C to be amorphous. The second step mass loss is in satisfactory agreement with the calculated value, assuming the product to have the Re<sub>2</sub>Ta<sub>4</sub>O<sub>12</sub> composition 23.8%. The X-ray powder study showed this product to be crystalline (see Figure 3), the second decomposition stage being thus associated with crystallization accompanied by extra oxygen loss.

The X-ray diffraction patterns of the L-Ta<sub>2</sub>O<sub>5</sub> and the rhenium–tantalum oxide phase have some common features, demonstrating the pronounced resemblance to

each other: most of the X-ray reflections of the rhenium–tantalum oxide phase, including all the strong ones, are present in the pattern of L-Ta<sub>2</sub>O<sub>5</sub> and have the same Miller indices, but the intensity distribution differs for the patterns in question. The other important difference is the smaller unit cell dimensions for the rhenium–tantalum oxide phase compared to those for L-Ta<sub>2</sub>O<sub>5</sub>.

The pattern of the rhenium–tantalum oxide phase can also be indexed with a reduced *b* parameter: the value *b* = 29.150(23) Å can be considered as the 8 times subcell dimension of the L-Ta<sub>2</sub>O<sub>5</sub> structure. (*b* = 3.644 × 8 ≈ 29.15 Å). Such multiplicity of 8 times the subcell is the lowest for the known structures derived from that of L-Ta<sub>2</sub>O<sub>5</sub> and was reported previously for the 15Ta<sub>2</sub>O<sub>5</sub>·2WO<sub>3</sub> phase and for the structure of L-Nb<sub>2</sub>O<sub>5</sub>.<sup>15,16</sup> In the case of the indexing of the rhenium–tantalum oxide X-ray pattern in the parameters similar to those of the L-Ta<sub>2</sub>O<sub>5</sub> phase, the *b* dimension turns out to be 11 times the subcell (*b* = 3.644 × 11 ≈ 40.08 Å compared to *b* = 3.664 × 11 ≈ 40.30 Å for L-Ta<sub>2</sub>O<sub>5</sub>).

Unlike that of **II**, the X-ray diffraction patterns of the decomposition products of **III** in the inert and the oxidizing atmospheres at 900 °C do not display common features, and the rhenium–niobium oxide phase is more likely to be derived from the L-Nb<sub>2</sub>O<sub>5</sub> structure<sup>16</sup> rather than from its high-temperature form.

It should be noted that the phases based on niobium and tantalum oxides are not simple objects for the powder X-ray diffraction study because of the rather complicated structural features and phase relations in the systems in question. In addition, the peaks of the X-ray diffraction patterns are somewhat broadened because of the fine grain size of the products obtained by the thermal decomposition of alkoxide complexes. These obstacles do not permit therefore an unequivocal indexing and interpretation of the X-ray patterns, including the determination of the true unit cell dimensions, without further structural investigations. Nevertheless, there are some conclusions that can be derived using the results obtained.

(15) Stephenson, N. C.; Roth, R. S. *Acta Crystallogr.* **1971**, B27, 1110.

(16) Waring, J. L.; Roth, R. S.; Parker, H. S. *J. Res. NBS* **1973**, 77A, 705.

## Conclusions

The synthetic approach to the new rhenium–niobium methoxide complex,  $\text{Nb}_2(\text{OMe})_8(\text{ReO}_4)_2$  (**III**), has been developed. This complex is formed upon interaction between  $\text{Re}_2\text{O}_7$  and the toluene solution of  $\text{Nb}_2(\text{OMe})_{10}$  and represents structurally the product of substitution for the terminal methoxo groups at each Nb atom in the dimeric  $\text{Nb}_2(\text{OMe})_{10}$  molecules with two perrhenate groups.

The decomposition of  $\text{Ta}_4\text{O}_2(\text{OMe})_{14}(\text{ReO}_4)_2$  (**II**) in an inert atmosphere at 900 °C provides the synthesis route to the rhenium–tantalum heterometallic oxide phase with the structure related presumably to the L- $\text{Ta}_2\text{O}_5$  phase structure. The decomposition of  $\text{Nb}_2(\text{OMe})_8(\text{ReO}_4)_2$  (**III**) under similar conditions leads to the formation of the rhenium–niobium oxide phase.

The results obtained provide the basis for the application of the alkoxide compounds in the synthesis of

the oxide materials containing rhenium, niobium, and tantalum using the “soft” chemistry approach.

**Acknowledgment.** The authors express their gratitude for financial support of this work to the Swedish Council for Natural Science Research, the Swedish Royal Academy of Sciences, the Russian Foundation for Basic Research (Project 0-03-32527), and the Ministry of Education of Russian Federation (Project 1“V”-27-871).

**Supporting Information Available:** Calculated XRD powder patterns for  $\text{Nb}_4\text{O}_2(\text{OMe})_{14}(\text{ReO}_4)_2$  (**I**),  $\text{Ta}_4\text{O}_2(\text{OMe})_{14}(\text{ReO}_4)_2$  (**II**), and  $\text{Nb}_2(\text{OMe})_8(\text{ReO}_4)_2$  (**III**) (PDF). Crystal data and details of diffraction experiment; atomic coordinates and equivalent isotropic displacement parameters for non-hydrogen atoms, and bond lengths and angles for **III** (PDF) and X-ray crystallographic file (CIF). XRD powder data for decomposition products of **II** and **III** (PDF). This material is available free of charge via the Internet at <http://pubs.acs.org>.

CM011726C